Electronic Supplementary Information

High-yield Synthesis and Acid-base Response of Phosphate-templated [3]Rotaxanes

Bo Qiao, Yun Liu, Semin Lee, Maren Pink, and Amar H. Flood*

Department of Chemistry, Indiana University, 800 East Kirkwood Avenue,

Bloomington, IN 47405, USA

S1. General Methods

Reagents were obtained from commercial suppliers and used as received unless otherwise noted. Building blocks used in the rotaxane synthesis, cyanostar (**CS**), tetrabutylammonium di(propargyl) phosphate (TBA•**P-C3**), tetrabutylammonium di(but-3-yn-1-yl) phosphate (TBA•**P-C4**), and dimethyl 5-azidoisophthalate were prepared according to reported procedures.[1,2] Ligand used in the copper-catalyzed alkyne-azide cycloadditions (CuAAC), tris-[(1-benzyl-1*H*-1,2,3-triazol-4-yl)methyl]amine (TBTA) was prepared according to reported procedures.[3] Column chromatography was performed on silica gel (160–200 mesh, SiliCycle Inc., Canada). Thin-layer chromatography (TLC) was performed on pre-coated silica gel plates (0.25 mm thick, SiliCycle Inc., Canada) and observed under UV light. Nuclear magnetic resonance (NMR) spectra were recorded on Varian Inova (600 MHz, 500 MHz, and 400 MHz) and Varian VXR (400 MHz) spectrometers at room temperature (298 K). Chemical shifts were referenced on residual solvent peaks. High-resolution electrospray ionization mass spectroscopy (HR-ESI-MS) was performed on a Thermo Electron Corporation MAT 95XP-Trap mass spectrometer.

S2. Syntheses and Compound Characterizations

List of abbreviations

TBA	Tetrabutylammonium
DBU	1,8-Diazabicycloundec-7-ene
TBTA	Tris-[(1-benzyl-1*H*-1,2,3-triazol-4-yl)methyl]amine
TEA	Triethylamine, Et_3N
TFA	Trifluoroacetic acid

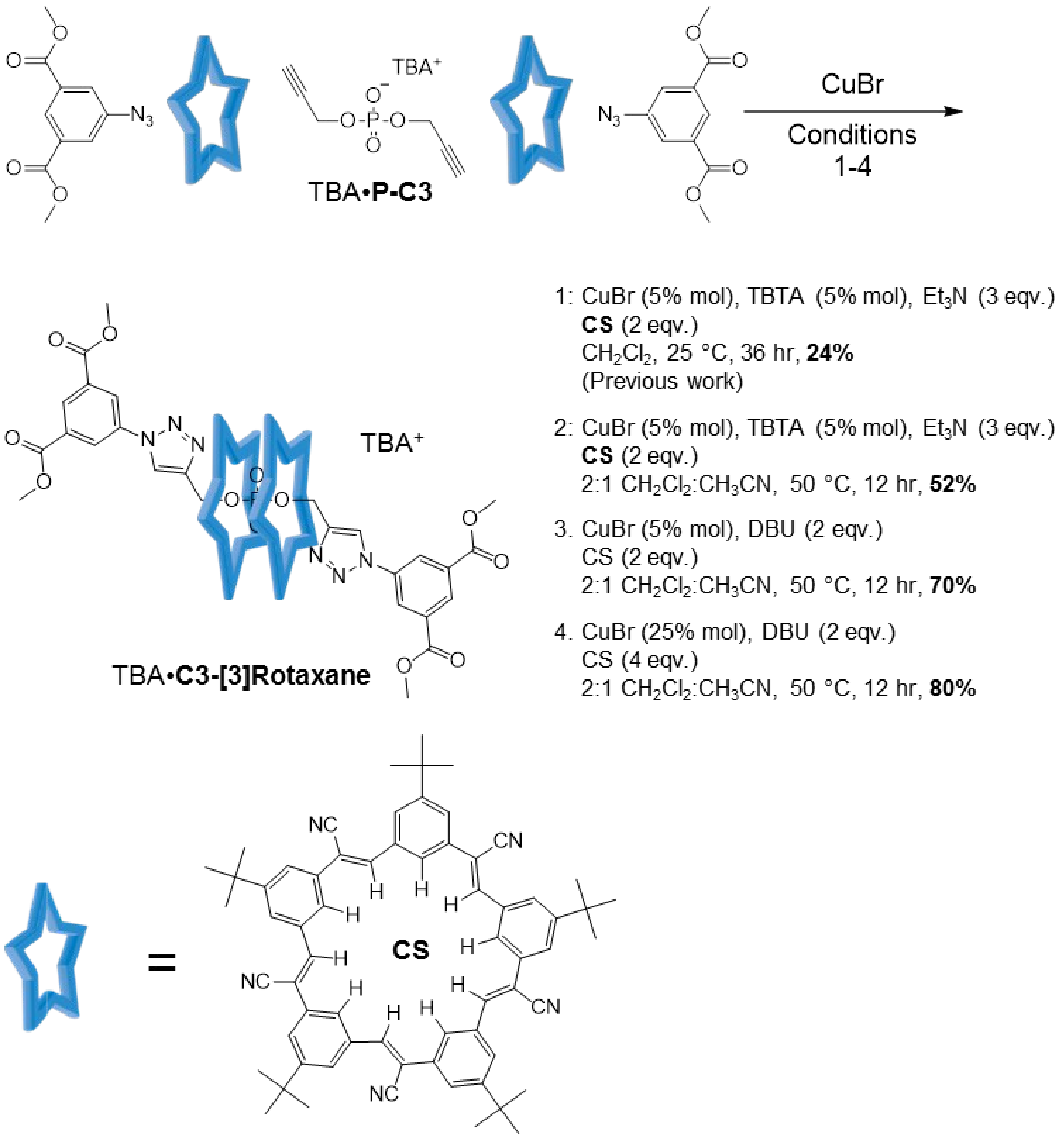

1: CuBr (5% mol), TBTA (5% mol), Et_3N (3 eqv.) **CS** (2 eqv.) CH_2Cl_2, 25 °C, 36 hr, **24%** (Previous work)

2: CuBr (5% mol), TBTA (5% mol), Et_3N (3 eqv.) **CS** (2 eqv.) 2:1 CH_2Cl_2:CH_3CN, 50 °C, 12 hr, **52%**

3. CuBr (5% mol), DBU (2 eqv.) CS (2 eqv.) 2:1 CH_2Cl_2:CH_3CN, 50 °C, 12 hr, **70%**

4. CuBr (25% mol), DBU (2 eqv.) CS (4 eqv.) 2:1 CH_2Cl_2:CH_3CN, 50 °C, 12 hr, **80%**

Scheme S1. Synthesis of TBA•**C3-[3]rotaxane**.

The previously reported synthesis of the cyanostar based TBA•**C3-[3]rotaxane** (condition 1)[1] employs CuBr as the catalyst, TBTA as the ligand, and Et_3N as the base. The reaction was carried out in CH_2Cl_2 at room temperature for 36 hours and gave a 24% yield. In this work, we conducted the reaction using the same substrates and catalyst but under optimized conditions (see below). The [3]rotaxane produced by the new conditions was characterized by ^1H NMR and ESI-MS, and the results matched previously reported spectra. The ^1H NMR spectrum of the TBA•**C3-[3]rotaxane** product can be found in Section S3.

Condition 2: Cyanostar (300 mg, 0.33 mmol), tetrabutylammonium di(propargyl) phosphate (68 mg, 0.16 mmol), dimethyl 5-azidoisophthalate (77 mg, 0.33 mmol), CuBr (2.3 mg, 5% mol), and TBTA (8.7 mg, 5% mol) were placed in a round bottom flask. The flask was degassed with argon. A degassed solution of Et_3N (100 mg, 140 µL, 1 mmol) in 2:1 CH_2Cl_2:CH_3CN (20 mL + 10 mL) was added to the flask via syringe. The reaction mixture was stirred at 50 °C for 12 h and concentrated in vacuo. The crude product was purified using column chromatography over silica gel (5% acetone in CH_2Cl_2) to yield TBA•**C3-[3]rotaxane** (230 mg, 8.4 mmol, 52% yield) as a white solid. ^{1}H NMR and ESI-MS of the product match the literature.

Condition 3: Cyanostar (300 mg, 0.33 mmol), tetrabutylammonium di(propargyl) phosphate (68 mg, 0.16 mmol), dimethyl 5-azidoisophthalate (77 mg, 0.33 mmol), and CuBr (2.3 mg, 5% mol) were placed in a round bottom flask. The flask was degassed with argon. A degassed solution of DBU (100 mg, 100 µL, 0.66 mmol) in 2:1 CH_2Cl_2 : CH_3CN (20 mL + 10 mL) was added to the flask via syringe. The reaction mixture was stirred at 50 °C for 12 h and concentrated in vacuo. The crude product was purified using column chromatography over silica gel (5% acetone in CH_2Cl_2) to yield TBA•**C3-[3]rotaxane** (300 mg, 0.11 mmol, 70% yield) as a white solid. ^{1}H NMR and ESI-MS of the product match the spectra in the literature.

Condition 4: Cyanostar (530 mg, 0.58 mmol), tetrabutylammonium di(propargyl) phosphate (60 mg, 0.14 mmol), dimethyl 5-azidoisophthalate (80 mg, 0.34 mmol), and CuBr (10 mg, 25% mol) were placed in a round bottom flask. The flask was degassed with argon. A degassed solution of DBU (110 mg, 110 µL, 0.72 mmol) in 2:1 CH_2Cl_2 : CH_3CN (20 mL + 10 mL) was added to the flask via syringe. The reaction mixture was stirred at 50 °C for 12 h and concentrated in vacuo. The crude product was purified using column chromatography over silica gel (5% acetone in CH_2Cl_2) to yield TBA•**C3-[3]rotaxane** (314 mg, 0.11 mmol, 80% yield) as a white solid. ^{1}H NMR and ESI-MS of the product match the spectra in the literature.

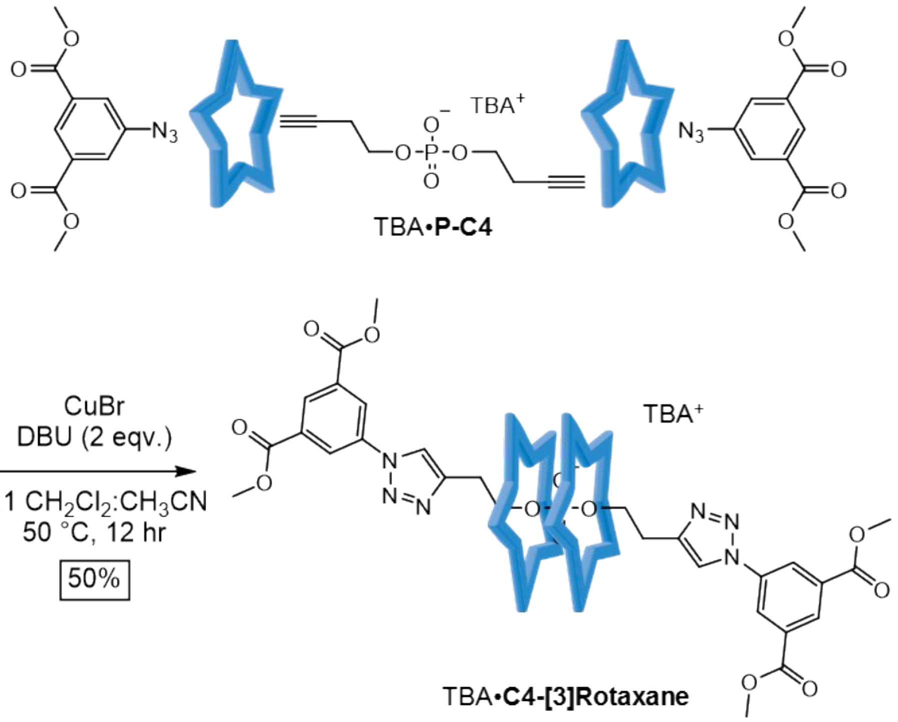

Scheme S2. Synthesis of TBA•**C4-[3]rotaxane**.

TBA•C4-[3]Rotaxane: Cyanostar (300 mg, 0.33 mmol), tetrabutylammonium di(but-3-yn-1-yl) phosphate (71 mg, 0.16 mmol), dimethyl 5-azidoisophthalate (77 mg, 0.33 mmol), and CuBr (2.3 mg, 5% mol) were placed in a round bottom flask. The flask was degassed with argon. A degassed solution of DBU (100 mg, 100 µL, 0.66 mmol) in 2:1 CH_2Cl_2:CH_3CN (20 mL + 10 mL) was added to the flask via syringe. The reaction mixture was stirred at 50 °C for 12 h and concentrated in vacuo. The crude product was purified using column chromatography over silica gel (5% acetone in CH_2Cl_2) to yield TBA•**C4-[3]rotaxane** (220 mg, 0.08 mmol, 50% yield) as a white solid. The rotaxane product is a mixture of two diastereomers (*PM* + *MP* and *MM* + *PP*) resulting from the prochirality of cyanostar.[1] The ratio between the major meso (*PM* + *MP*) and the minor chiral (*MM* + *PP*) diastereomers is ~2:1 as determined by ^{1}H NMR integration.

^{1}H NMR of the meso diastereomer (CD_2Cl_2, 600 MHz), δ = 8.39 (t, J = 1 Hz, 2H), 8.18 (s, 10H), 8.13 (s, 20H), 7.94 (d, J = 1 Hz, 4H), 7.59 (s, 10H), 7.47 (s, 2H), 5.20 (m, 4H), 3.80 (s, 12H), 3.49 (m, 4H), 2.99 (m, 8H), 1.54 (s, 90H), 1.30 (sextet, J = 7.4 Hz, 8H), 0.91 (t, J = 7.3 Hz, 12H).

^{1}H NMR of the chiral diastereomer (CD_2Cl_2, 600 MHz), δ = 8.40 (s, 10H), 8.37 (t, J = 1 Hz, 2H), 8.15 (s, 10H), 8.11 (s, 10H), 7.88 (d, J = 1 Hz, 4H), 7.51 (s, 2H), 7.44 (s, 10H), 5.20 (m, 4H), 3.80 (s, 12H), 3.43 (m, 4H), 2.99 (m, 8H), 1.52 (s, 90H), 1.30 (sextet, J = 7.4 Hz, 8H), 0.91 (t, J = 7.3 Hz, 12H).

^{13}C NMR of the two diastereomers (CD_2Cl_2, 100 MHz), δ = 164.6, 152.8, 152.7, 144.5, 141.8, 141.7, 136.6, 134.3, 134.2, 133.9, 133.8, 132.1, 132.0, 129.4, 126.6, 126.4, 125.9, 123.6, 123.4, 123.3, 123.0, 119.4, 117.7, 117.6, 65.1, 59.0, 53.4, 35.4, 31.1, 23.7, 19.6, 13.2.

HR-EI-MS: $C_{158}H_{158}N_{16}O_{12}P^-$ [M − TBA]$^-$, Calculated: 2502.1982, Found: 2502.1960.

S3. ^{1}H and ^{13}C NMR Spectra

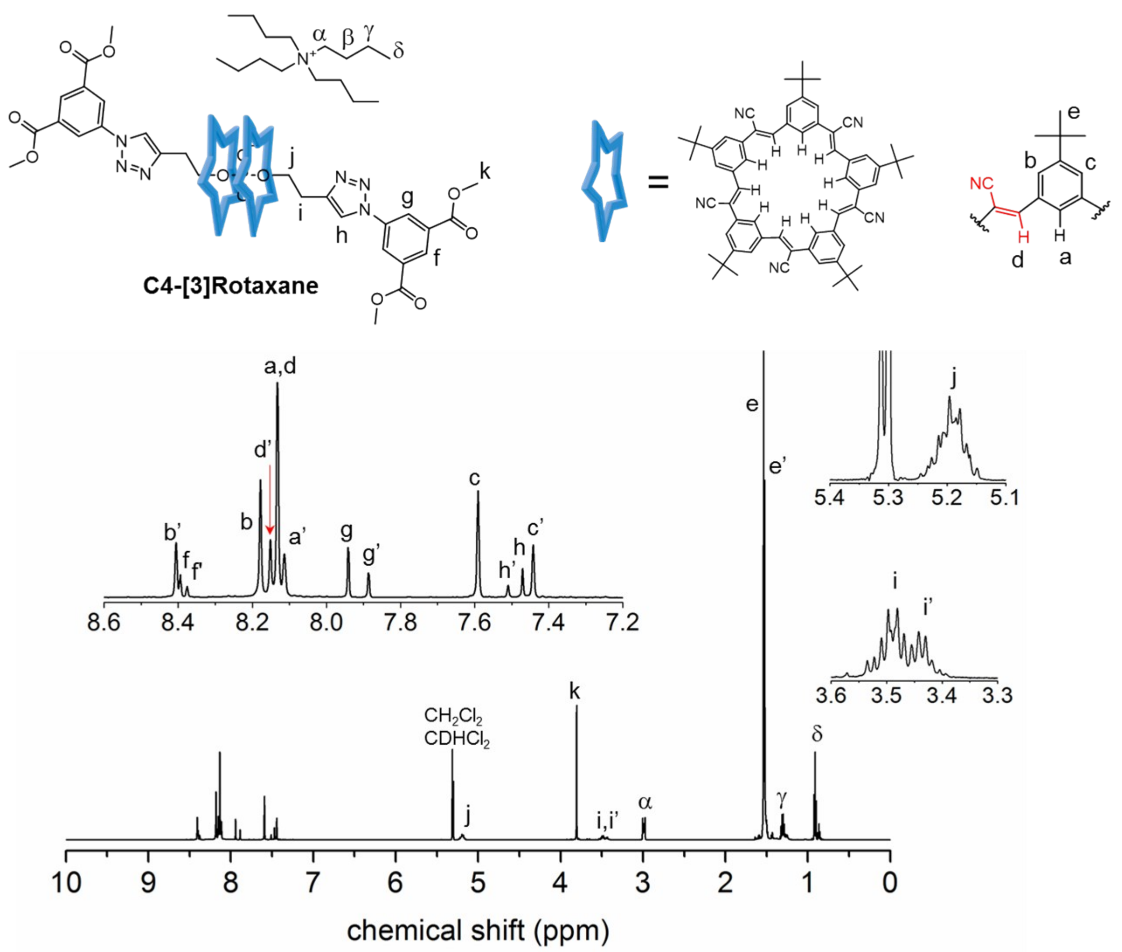

Figure S1. ^{1}H NMR spectrum of TBA•**C4-[3]rotaxane** (’ donates peaks from the minor diastereomer).

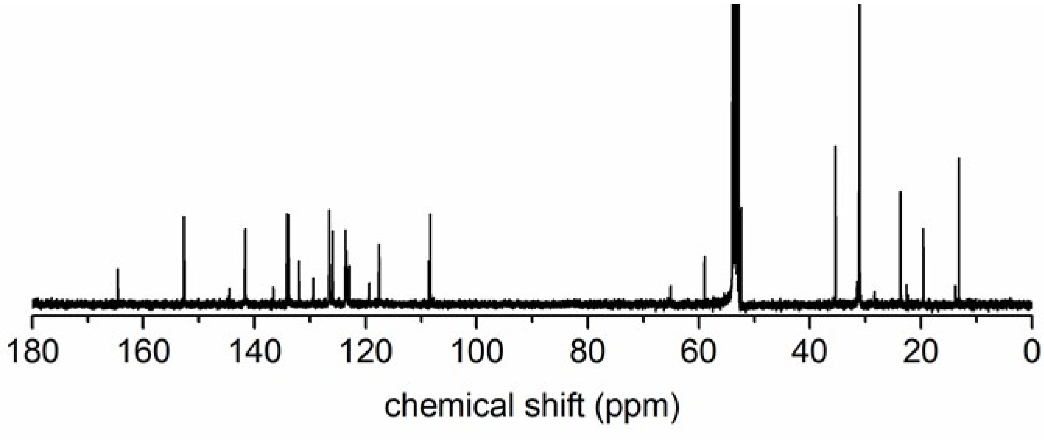

Figure S2. ^{13}C NMR spectrum of TBA•**C4-[3]rotaxane**.

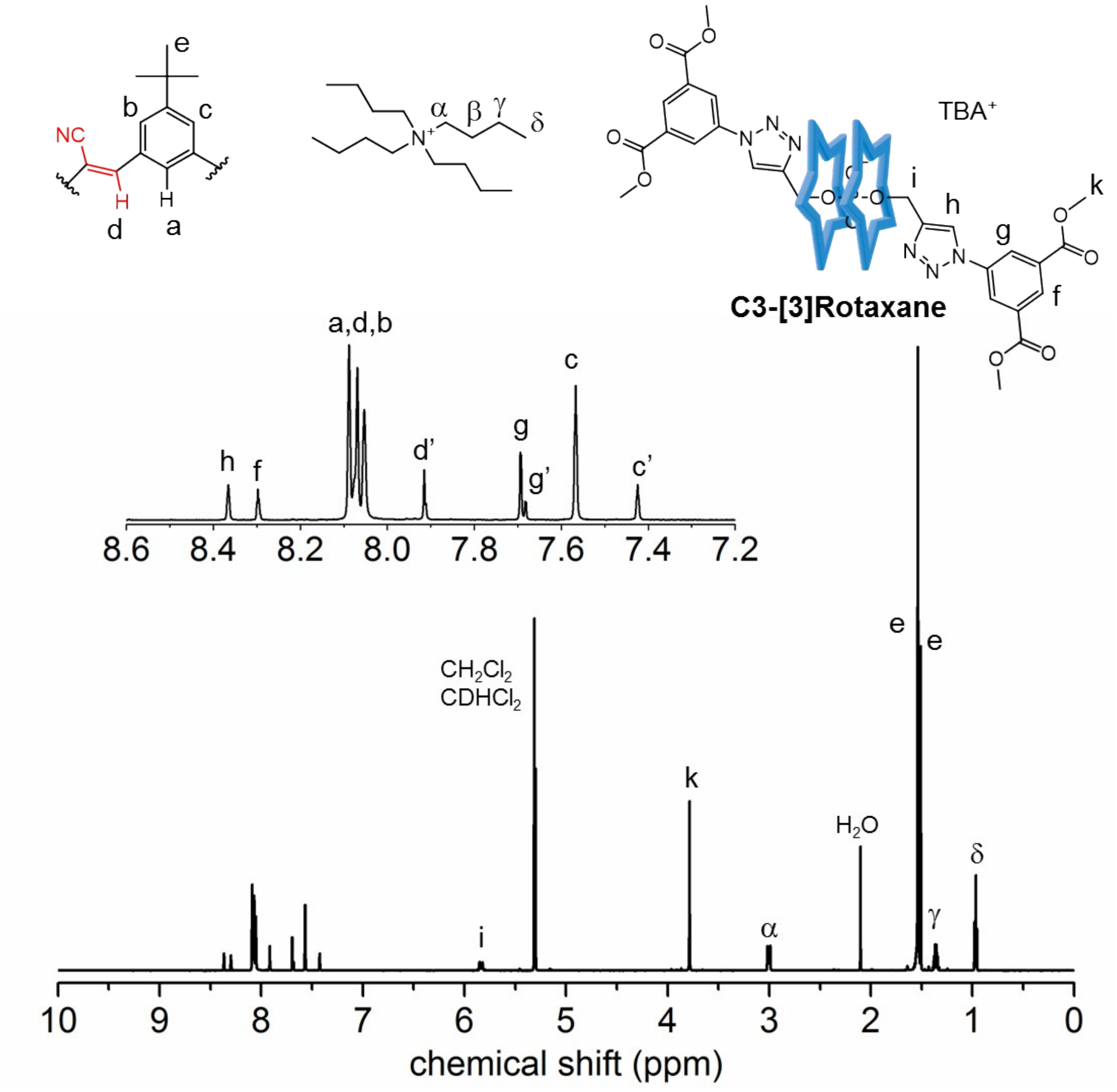

***Figure S3*.** ^{1}H NMR spectrum of TBA•**C3-[3]rotaxane** (’ donates peaks from the minor diastereomer).

S4. 2D NMR Spectroscopy of TBA•C4-[3]Rotaxane

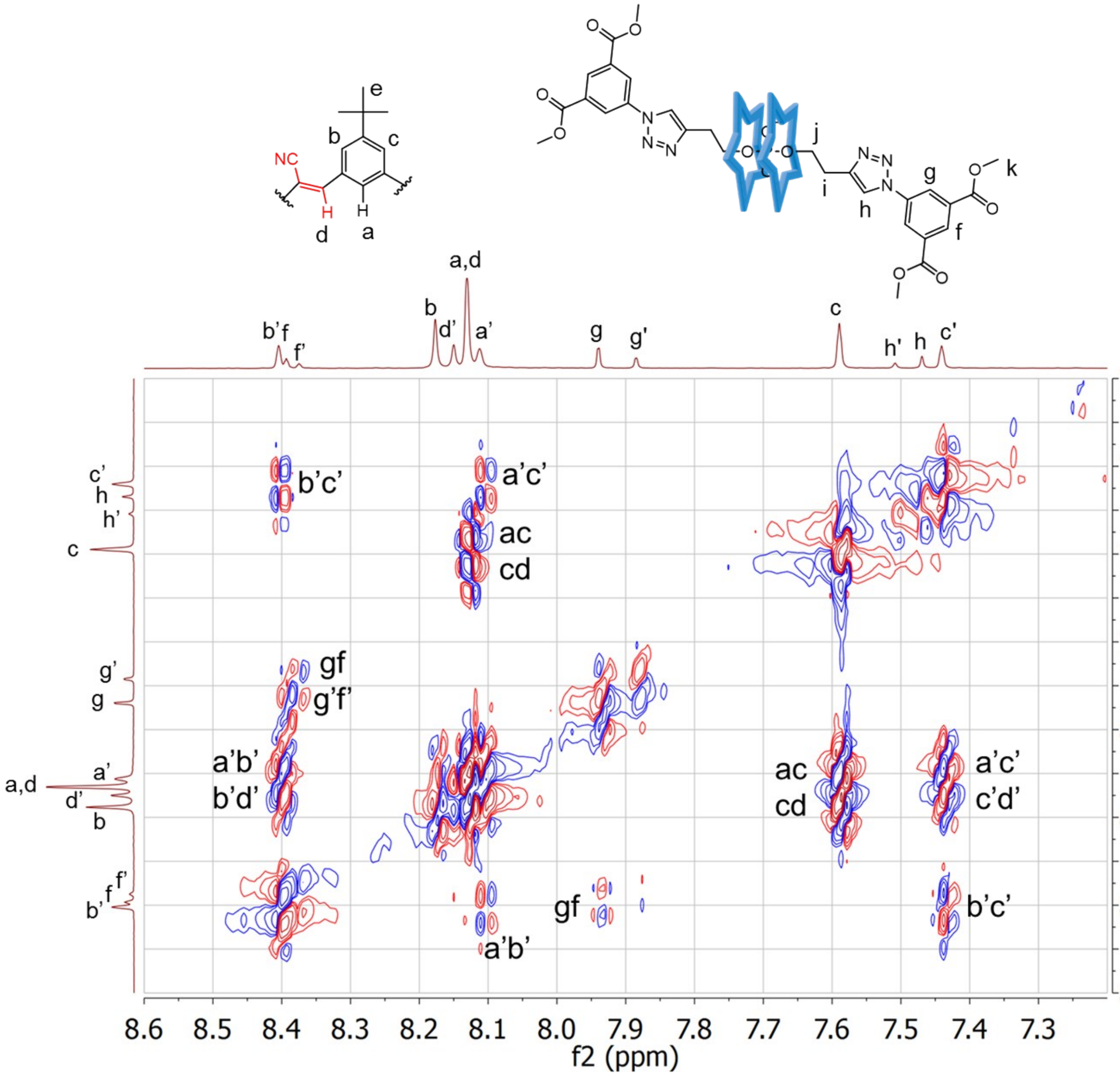

Figure S4. ^{1}H-^{1}H Through-bond coupling DQF-COSY NMR spectrum of TBA**•C4-[3]rotaxane** (CD_2Cl_2, 600 MHz), shows cross peaks for separate spin systems of the major and minor (’) diastereomers.

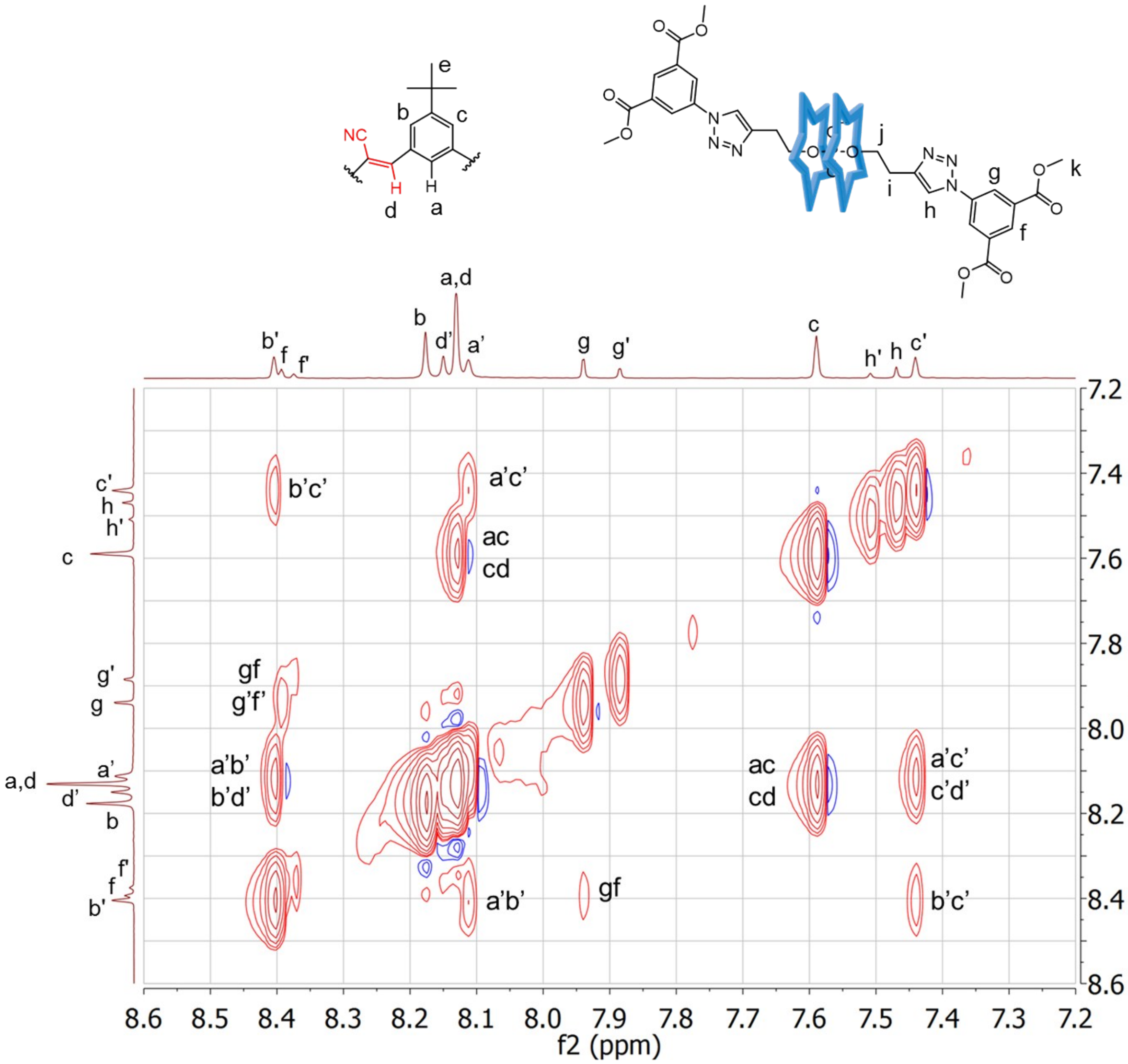

Figure S5. ^{1}H-^{1}H Through-bond coupling TOCSY NMR spectrum of TBA•**C4-[3]rotaxane** (CH_2Cl_2, 600 MHz) shows cross peaks for separate spin systems of the major and minor (’) diastereomers.

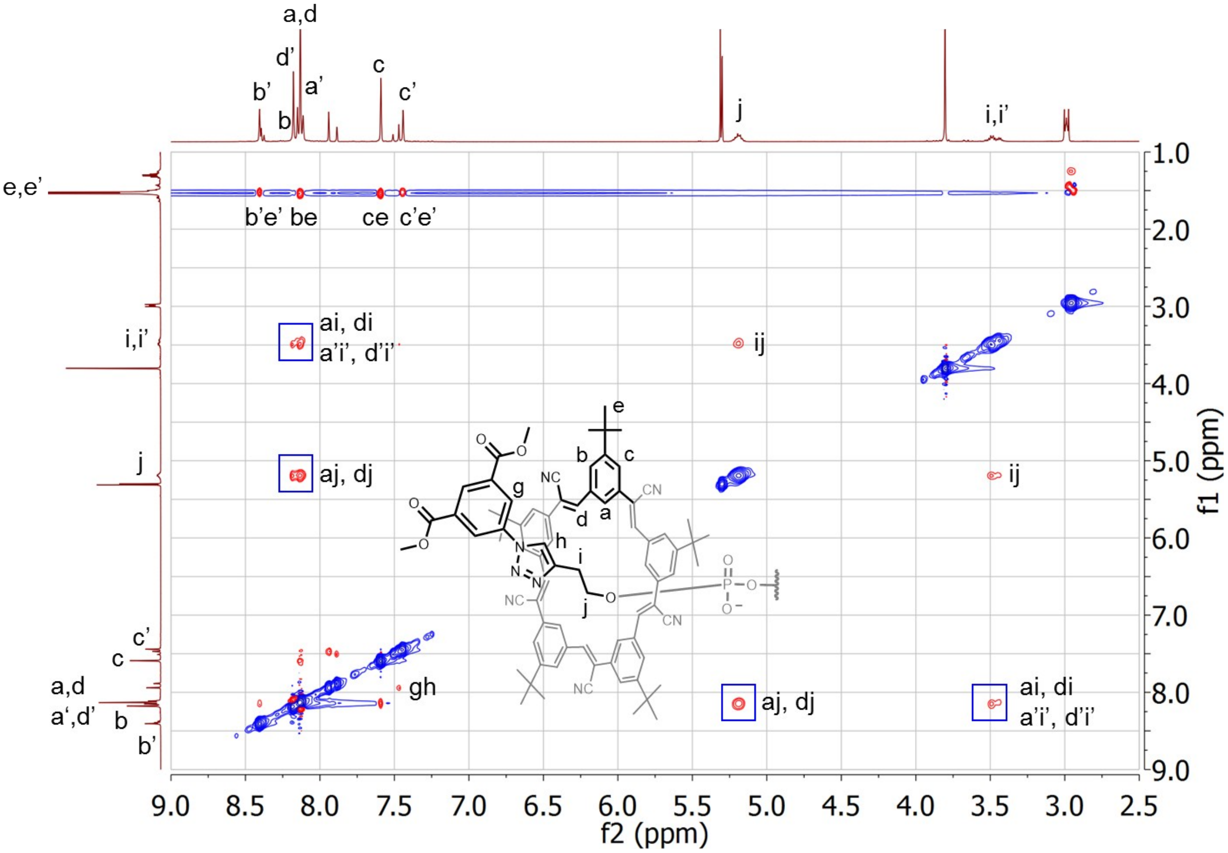

Figure S6. ^{1}H-^{1}H Through-space ROESY NMR spectrum of TBA•**C4-[3]rotaxane** (CD_2Cl_2, 500 MHz, mixing time: 0.2 s), showing cross peaks between the cyanostars and the dumbbell (highlighted in blue boxes).

S5. Mass Spectroscopy of TBA•C4-[3]Rotaxane

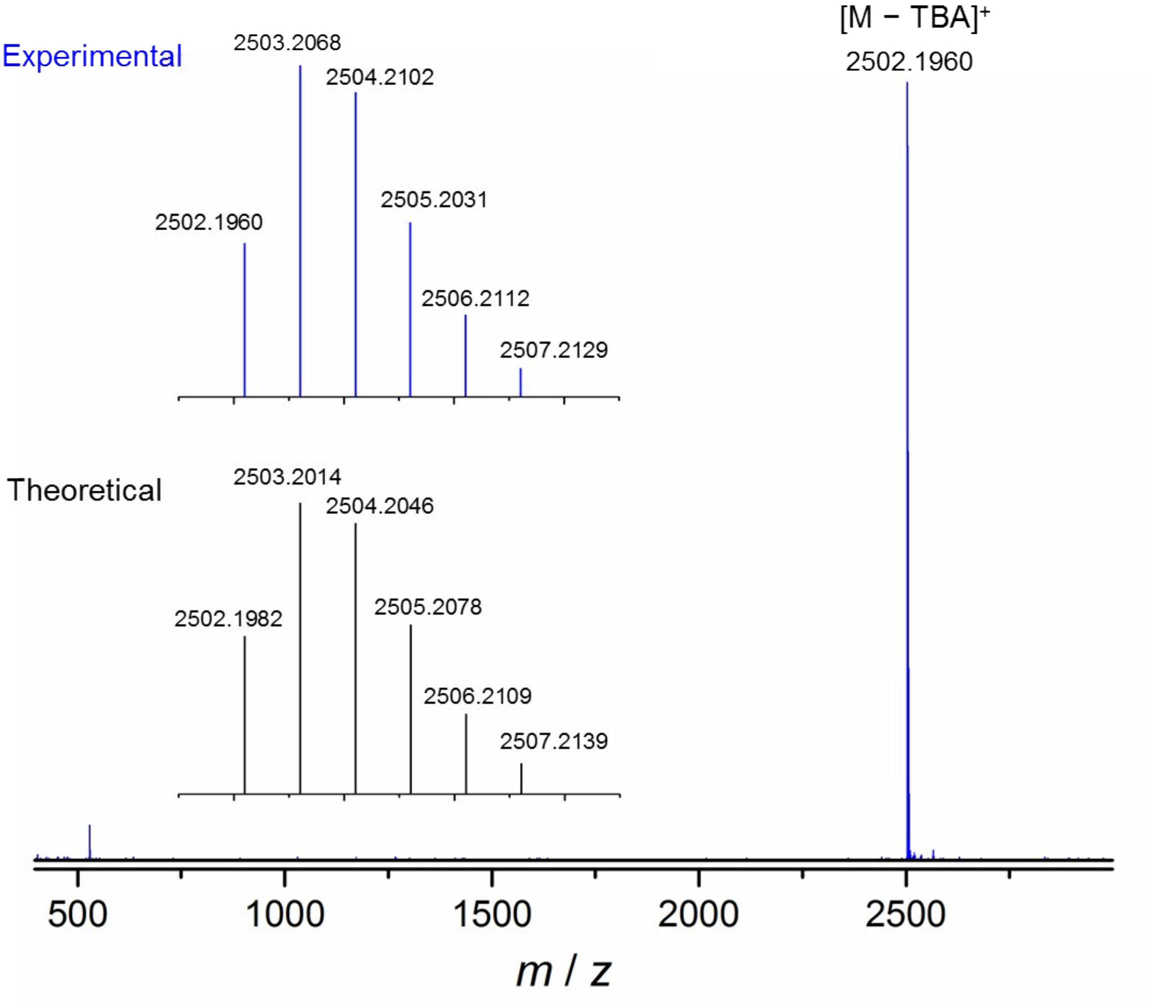

Figure S7. HR-ESI-MS of TBA•**C4-[3]rotaxane**.

S6. X-Ray Crystallography

S 6.1 X-Ray Diffraction Data Analysis of TBA•C4-[3]Rotaxane

Data Collection

The data collection was carried out using Mo Kα radiation (graphite monochromator) with a frame time of 60 seconds and a detector distance of 50 mm. Data to a resolution of approximately 0.84 Å could be obtained. A collection strategy was calculated and complete data to a resolution of 0.80 Å with a redundancy of 4 were collected. Nine major sections of frames were collected with 0.50° ω and ϕ scans; details are below.

Axis	**2θ/°**	**ω/°**	**φ/°**	**χ/°**	**Frames**
Phi	24.50	264.97	26.47	55.92	473
Omega	24.50	-18.08	-74.18	92.25	103
Phi	22.00	314.35	-308.63	65.90	554
Phi	9.50	19.07	-95.67	-46.47	161
Omega	32.00	-25.85	54.52	96.27	63
Omega	-18.00	-56.34	-17.50	57.63	96
Phi	24.50	16.38	-26.06	-55.24	739
Phi	27.00	298.11	-73.87	45.39	207
Omega	17.00	-38.44	-229.91	34.46	150

A total of 2546 frames were collected. The total exposure time was 22.56 hours. The frames were integrated with the Bruker SAINT software package[4] using a narrow-frame algorithm. The integration of the data using a monoclinic unit cell yielded a total of 61341 reflections to a maximum θ angle of 27.48° (0.77 Å resolution), of which 20734 were independent (average redundancy 2.958, completeness = 98.2%, R_{int} = 3.35%, R_{sig} = 4.54%) and 12081 (58.27%) were greater than $2\sigma(F_2)$. The final cell constants of a = 30.3787(16) Å, b = 19.6365(10) Å, c = 32.742(3) Å, β = 109.7191(13)°, volume = 18386.(2) Å^3, are based upon the refinement of the XYZ-centroids of 9947 reflections above 20 $\sigma(I)$ with 4.75° < 2θ < 54.42°. Data were corrected for absorption effects using the multi-scan method (SADABS).[5] The ratio of minimum to maximum apparent transmission was 0.827. The calculated minimum and maximum transmission coefficients (based on crystal size) are 0.6163 and 0.7456.

Structure Solution and Refinement

The space group C2/c was determined based on intensity statistics and systematic absences. The structure was solved and refined using the SHELX suite of programs.[6] An intrinsic-methods solution was calculated, which provided most non-hydrogen atoms from the E-map. Full-matrix least squares/difference Fourier cycles were performed, which located the remaining non-hydrogen atoms. All non-hydrogen atoms were refined with anisotropic displacement parameters. The hydrogen atoms were placed in ideal positions and refined as riding atoms with relative isotropic displacement parameters. Half of the formula unit is crystallographically unique. Disorder was refined for cyanostar, the phosphate and solvent chloroform. Restraints and constraints including rigid bond restraints, equal thermal displacement, similar distance were applied to obtain a stable and chemically reasonable model.

The final anisotropic full-matrix least-squares refinement on F_2 with 1304 variables converged at R_1 = 12.30%, for the observed data and wR_2 = 43.71% for all data. The goodness-of-fit was 1.223. The largest peak in the final difference electron density synthesis was 1.188 $e^{-}/Å^{3}$ and the largest hole was −0.890 $e^{-}/Å^{3}$ with an RMS deviation of 0.088 $e^{-}/Å^{3}$ On the basis of the final model, the calculated density was 1.251 g/cm^3 and F(000), 7264 e^{-}.

Table S1. Crystal data and structure refinement for TBA•**C4-[3]rotaxane**.

Empirical formula	$C_{180}H_{200}Cl_{18}N_{17}O_{12}P$	
Formula weight	3462.63	
Crystal color, shape, size	colorless block, 0.34 × 0.27 × 0.23 mm^3	
Temperature	220(2) K	
Wavelength	0.71073 Å	
Crystal system, space group	Monoclinic, C2/c	
Unit cell dimensions	a = 30.3787(16) Å	α = 90°.
	b = 19.6365(10) Å	β = 109.7191(13)°.
	c = 32.742(3) Å	γ = 90°.
Volume	18386(2) Å^3	
Z	4	
Density (calculated)	1.251 mg/m^3	
Absorption coefficient	0.338 mm^{-1}	
F(000)	7264	

Data collection

Diffractometer	APEX II Kappa Duo, Bruker
Theta range for data collection	1.258 to 27.484°.
Index ranges	$-39 \leq h \leq 39$, $-25 \leq k \leq 24$, $-42 \leq l \leq 38$
Reflections collected	61341
Independent reflections	20734 [R_{int} = 0.0335]
Observed Reflections	12081
Completeness to theta = 25.242°	99.1 %

Solution and Refinement

Absorption correction	Semi-empirical from equivalents
Max. and min. transmission	0.7456 and 0.6163
Solution	Intrinsic methods

Refinement method	Full-matrix least-squares on F^2
Weighting scheme	$w = [\sigma^2 F_o^2 + AP^2 + BP]^{-1}$, with $P = (F_o^2 + 2 F_c^2) / 3$, $A = 0.25$, $B = 12.0$
Data / restraints / parameters	20734 / 3206 / 1304
Goodness-of-fit on F^2	1.223
Final R indices [$I > 2\text{sigma}(I)$]	$R_1 = 0.1230$, $wR_2 = 0.3701$
R indices (all data)	$R_1 = 0.1777$, $wR_2 = 0.4371$
Largest diff. peak and hole	1.188 and −0.890 e•Å^{-3}

Goodness-of-fit = $[\Sigma[w(F_o^2 - F_c^2)^2] / N_{\text{observns}} - N_{\text{params}})]^{1/2}$, all data.

$R_1 = \Sigma(|F_o| - |F_c|) / \Sigma |F_o|$. $wR_2 = [\Sigma[w(F_o^2 - F_c^2)^2] / \Sigma [w(F_o^2)^2]]^{1/2}$.

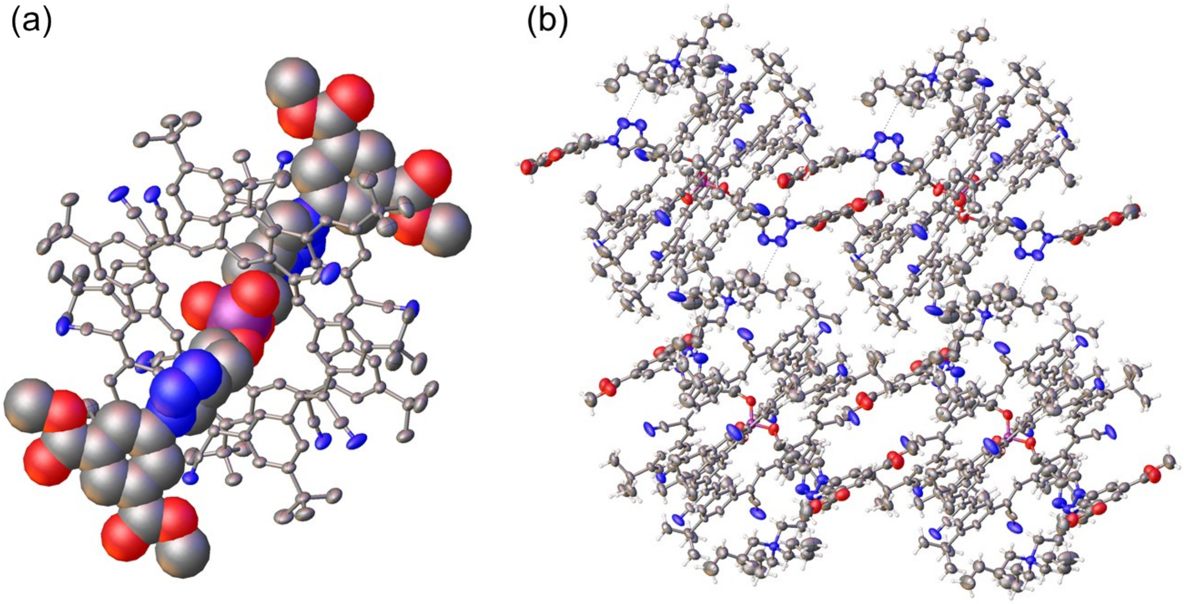

Figure S8. (a) The crystal structure of TBA•**C4-[3]rotaxane**. The dumbbell is displayed with van der Waals radii. Disorder, solvent molecules and cations are omitted. (b) The packing within the TBA•**C4-[3]rotaxane** crystal. Disorder, solvent molecules are omitted.

S 6.2 X-Ray Diffraction Data Analysis of the Pseudorotaxane TBA•[P-C3•CS$_2$]

Data collection

The data collection was carried out using Mo Kα radiation (graphite monochromator) with a frame time of 60 seconds and a detector distance of 7.00 cm. A collection strategy was calculated and complete data to a resolution of 0.80 Å with a redundancy of 4 were collected. Four major sections of frames were collected with 0.50º ω and ϕ scans. The total exposure time was 25.43 hours. Notably and as observed for most cyanostar structures that have been investigated in our laboratory,[1,7] diffraction terminates at low resolution even with excessive exposure times. The frames were integrated with the Bruker SAINT software package[4] using a narrow-frame algorithm. The integration of the data using a cubic unit cell yielded a total of 326554 reflections to a maximum θ angle of 25.06° (0.84 Å resolution), of which 14940 were independent (average redundancy 21.858, completeness = 99.9%, R_{int} = 21.19%, R_{sig} = 6.18%) and 8451 (56.57%) were greater than $2\sigma(F2)$. The final cell constants of a = 36.9585(19) Å, b = 36.9585(19) Å, c = 36.9585(19) Å, volume = 50483.(8) Å^3, are based upon the refinement of the XYZ-centroids of 9767 reflections above 20 $\sigma(I)$ with 4.544° < 2θ < 48.15°. Data were corrected for absorption effects using the multi-scan method (SADABS).[5] The ratio of minimum to maximum apparent transmission was 0.727. The calculated minimum and maximum transmission coefficients (based on crystal size) are 0.9870 and 0.9900.

Structure Solution and Refinement

The space group P4$_3$32 was determined based on intensity statistics and systematic absences. The structure was solved and refined using the SHELX suite of programs.[6] An intrinsic-methods solution was calculated, which provided most non-hydrogen atoms of cyanostar and including disorder sites from the E-map. Full-matrix least squares/difference Fourier cycles were performed, which located the remaining non-hydrogen atoms. All non-hydrogen atoms were refined with anisotropic displacement parameters with rigid bond restraints. The hydrogen atoms were placed in ideal positions and refined as riding atoms with relative isotropic displacement parameters. Remaining electron density indicates a phosphate moiety threaded through two cyanostars and located on a special position.

The structure clearly shows the formation of [3]pseudorotaxane, however further refinement was not successful on account of multiple instances of whole molecular disorder. As a means to address the disorder, two complementary strategies were followed. The first uses aggressive restraints and constraints while the second employs the SQUEEZE algorithm.

First, the alkyl arms of the phosphate appear to be disordered and coupled with multiple sites of TBA$^+$, both of which located on a special position. While the refinement of the disordered phosphate core is successful (R_1 = 0.21, highest difference electron density 1.4 e/Å^3), the alkyl arms and the counter cation refinement fails despite the use of excessive restraints and constraints (chemically sensible geometry and convergence can be achieved).

Second, the structure was investigated for solvent accessible areas using SQUEEZE[8]. However, on account of the correlated disorder and close proximity of the cation and anion, the whole TBA•**P-C3** ion pair was removed by the SQUEEZE function. The total void space (per unit cell) is 21236 Å^3 (42% of the unit cell) containing 6563 electrons. That is per cyanostar dimer, the void space and electron count is 1770 Å^3 and 547, respectively. For comparison, TBA^+ occupies ca. 431 Å^3 with 139 electrons and $PO_4C_6H_6$, 196 Å^3 with 89 electrons.[9] The contribution of the unidentified ion pair and possibly solvent to the structure factors was assessed by inverse Fourier transformation and the data were modified accordingly. The refinement using the modified dataset improved the overall structure and R_1 by about 10 %. The final anisotropic full-matrix least-squares refinement of the model with modified F_2 and 722 variables converged at R_1 = 11.18%, for the observed data and wR_2 = 29.50% for all data. The goodness-of-fit was 1.587. The largest peak in the final difference electron density synthesis was 0.292 e$^-$/Å^3 and the largest hole was −0.292 e$^-$/Å^3 with an RMS deviation of 0.060 e$^-$/Å^3. On the basis of the final model, the calculated density is 0.723 g/cm^3 and F(000), 11760 e$^-$.

Table S2. Crystal data and structure refinement for TBA•[P-C3•CS$_2$] with TBA•P-C3 ion pair excluded

Empirical formula	$C_{130}H_{130}N_{10}$	
Formula weight	1832.43	
Crystal color, shape, size	colorless block, 0.310 × 0.250 × 0.250 mm^3	
Temperature	230(2) K	
Wavelength	0.71073 Å	
Crystal system, space group	Cubic, $P4_332$	
Unit cell dimensions	a = 36.9585(19) Å	α = 90°.
	b = 36.9585(19) Å	β = 90°.
	c = 36.9585(19) Å	γ = 90°.
Volume	50483(8) Å^3	
Z	12 (based on CS dimer)	
Density (calculated)	0.723 mg/m^3	
Absorption coefficient	0.042 mm^{-1}	
F(000)	11760	
Data collection		
Diffractometer	APEX II Kappa Duo, Bruker	
Theta range for data collection	1.232 to 25.056°.	
Index ranges	$-43 \le h \le 44$, $-43 \le k \le 39$, $-44 \le l \le 26$	
Reflections collected	326554	
Independent reflections	14940 [R(int) = 0.2119]	

Observed Reflections	8451
Completeness to theta = 25.056°	100.0 %

Solution and Refinement

Absorption correction	Semi-empirical from equivalents
Max. and min. transmission	0.7452 and 0.5420
Solution	Intrinsic methods
Refinement method	Full-matrix least-squares on F^2
Weighting scheme	$w = [\sigma^2 F_o^2 + 0.1000\ P^2]^{-1}$, with $P = (F_o^2 + 2\ F_c^2) / 3$
Data / restraints / parameters	14940 / 2235 / 722
Goodness-of-fit on F^2	1.587
Final R indices [I>2sigma(I)]	$R_1 = 0.1118$, $wR_2 = 0.2719$
R indices (all data)	$R_1 = 0.1646$, $wR_2 = 0.2950$
Absolute structure parameter	0.8(5)
Largest diff. peak and hole	0.292 and −0.292 e Å^{-3}

Goodness-of-fit = $[\Sigma[w(F_o^2 - F_c^2)^2]/N_{observns} - N_{params})]^{1/2}$, all data.
R1 = $\Sigma(|F_o| - |F_c|) / \Sigma |F_o|$. wR2 = $[\Sigma[w(F_o^2 - F_c^2)^2] / \Sigma [w(F_o^2)^2]]^{1/2}$.

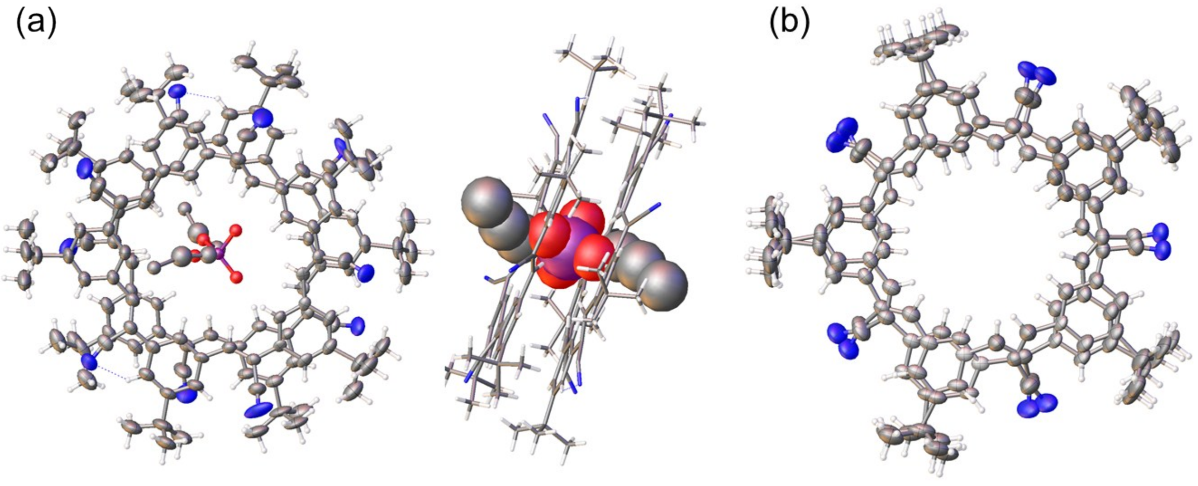

Figure S9. (a) Top and (b) side views of the partially refined structure showing the formation of [3]pseudorotaxane. This refinement fails on account of highly disordered TBA$^+$ cation and phosphate alkyl chains. (b) Fully refined crystal structure with TBA•**P-C3** ion pair excluded under SQUEEZE algorithm.

S7. ^{1}H NMR Titrations and Phosphate Binding Analyses

Methods

Titrations of dialkyl phosphates into cyanostar solutions proceeded as follows: A solution of cyanostar (500 µL, 1 mM) was placed in an NMR tube sealed with a rubber septum. An initial ^{1}H NMR spectrum was recorded and additional spectra were obtained after aliquots of tetrabutylammonium dialkyl phosphate (25 mM) was injected sequentially using a microsyringe.

Binding Data

The binding data of cyanostar with TBA•**P-C3** at room temperature (1 mM, CD_2Cl_2, 298 K) are included in the main text. Here we show the binding of cyanostar with TBA•**P-C4** at room temperature (1 mM, CD_2Cl_2, 298 K) and cyanostar with TBA•**P-C3** at higher temperature (1 mM, 2:1 CD_2Cl_2:CD_3CN, 323 K). The used of acetonitrile as a co-solvent allows the access to higher temperature.

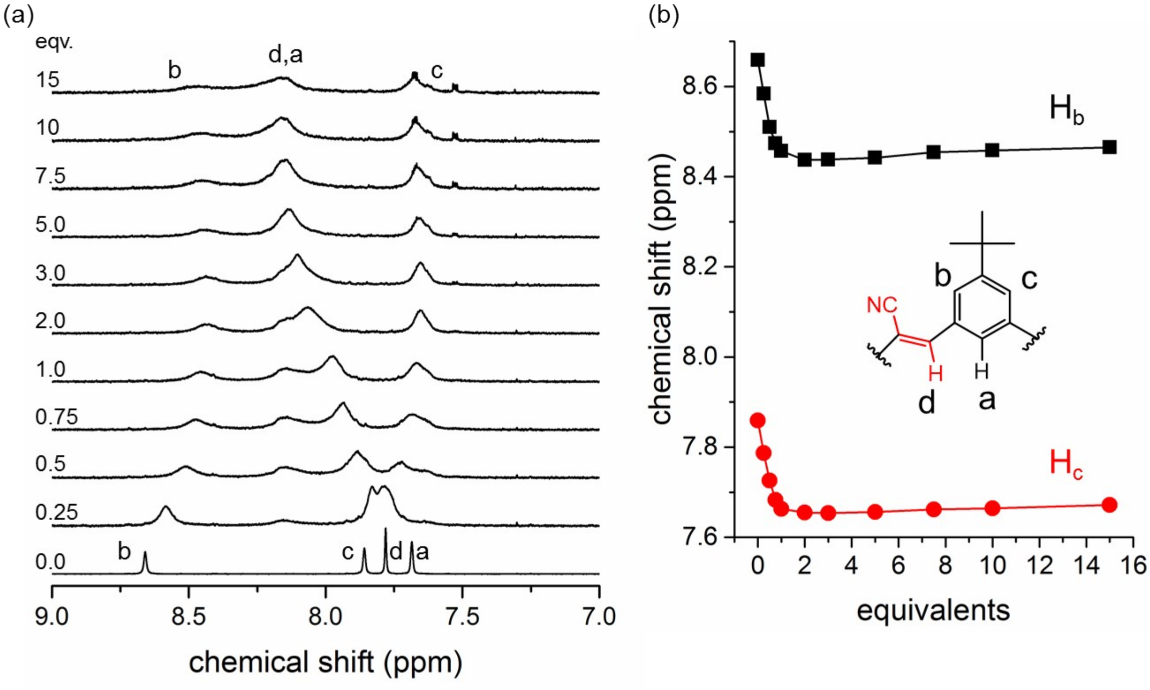

Figure S10. (a) Stacked ^{1}H NMR spectra and (b) chemical shift positions of cyanostar protons H_b and H_c connected by trend lines with increasing amount of TBA•**P-C4** (1 mM, CD_2Cl_2, 298 K, 600 MHz).

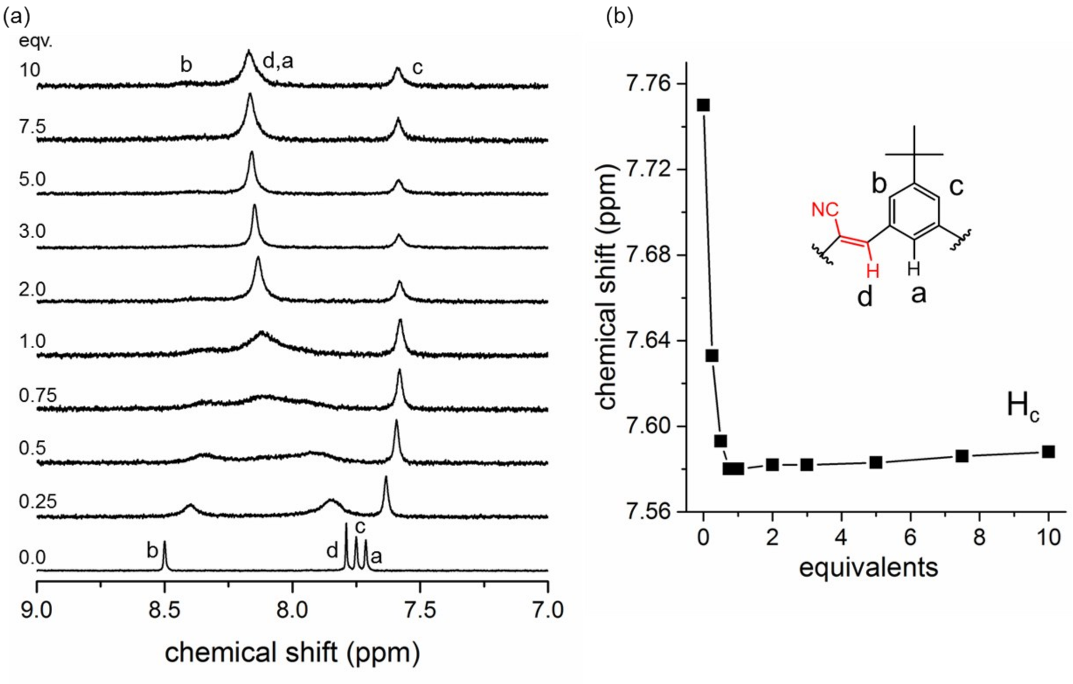

Figure S11. (a) Stacked ^{1}H NMR spectra and (b) chemical shift positions of cyanostar proton H_c connected by trend lines with increasing amount of TBA•**P-C3** (1 mM, 2:1 CD_2Cl_2:CD_3CN, 323 K, 600 MHz).

Modeling the 2:1 Complexes

The titration of TBA•**P-C3** into cyanostar shows strong 2:1 binding. Molecular mechanics (MMFF94 force field) was used to model various binding configurations for the 2:1 complexes formed between two cyanostars and one dialkyl phosphate. The [3]pseudorotaxane is the most stabilized configuration (Figure S12).

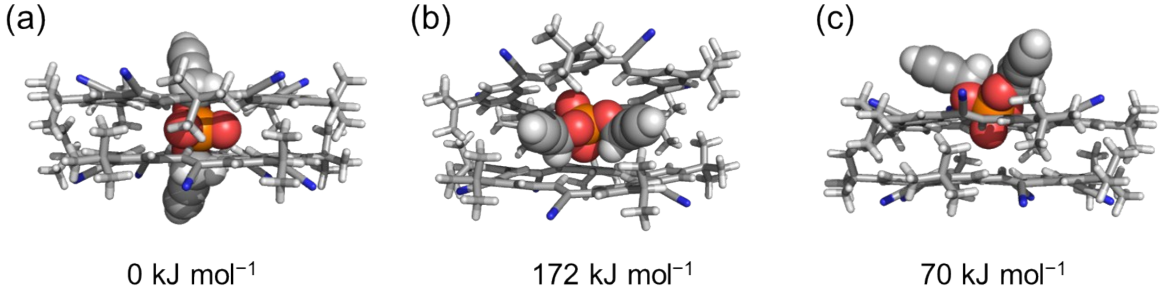

Figure S12. Molecular models and the relative energy of different 2:1 binding configurations determined by molecular mechanics

DFT Analysis on Deformation of Phosphate Threads

All computations in this section were carried out by density functional theory (DFT) computations using the M06-2X functional[S10] with Spartan ’14[S11]. Geometry optimizations were performed using the 6-31G(d) basis set in gas phase. Vibrational analysis was conducted to verify the stationary points to be minimum energy structures. Single-point energies were calculated at higher M06-2X/6-31+G(d,p) level of theory. The deformation energy was calculated as energy penalty from unbound to bound geometries.

The global minima of the free phosphate threads were identified by conformational search in Spartan ’14. The MMFF94 force field[12] was used for the initial search; increasingly accurate methods were subsequently used to optimize the conformational space: HF/3-21G and then M06-2X/6-31G(d). The geometries of the bound phosphate threads were taken from refined or partially refined crystal structures. These geometries were relaxed using M062X/6-31G(d) while the conformations were constrained to be consistent with crystal structures.

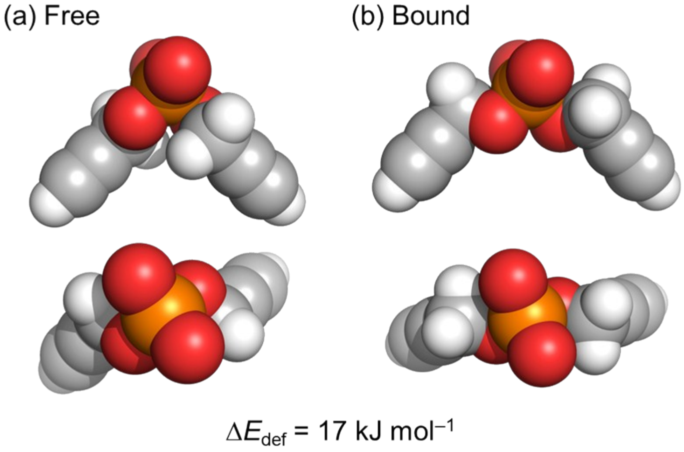

Figure S13. The most stable conformers of (a) free **P-C3**$^{-}$ and (b) **P-C3**$^{-}$ bound by two cyanostars (two views for each). The energy difference between the two conformers (deformation energy, ΔE_{def}) is marked in the figure.

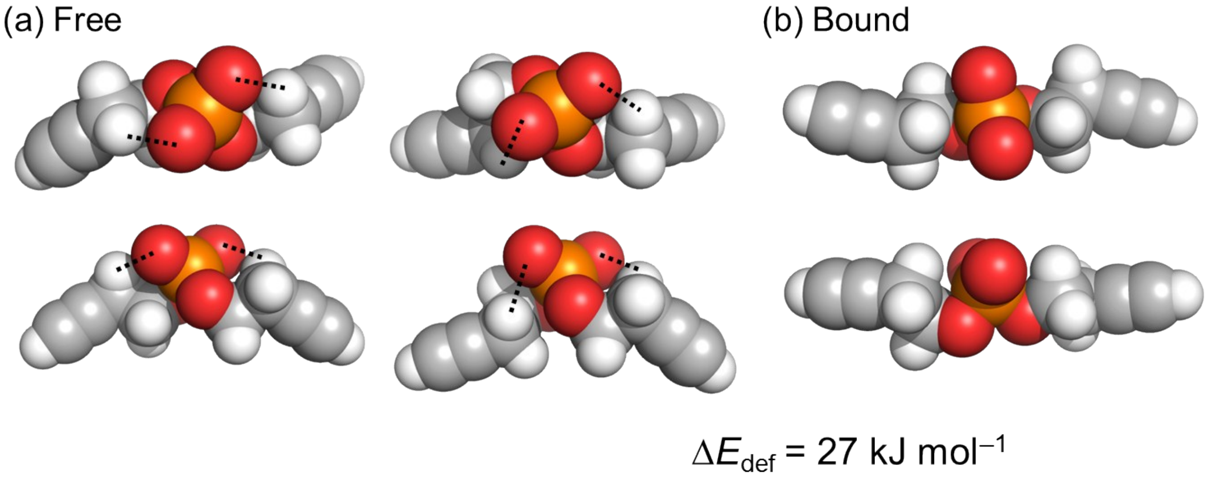

Figure S14. (a) The most stable conformers of (a) free **P-C4**$^-$ anion (four views) and (b) **P-C4**$^-$ bound by two cyanostars (two views). Attractive CH•••O interactions within the free anion are shown in black dashed lines. The energy difference between the two conformers (deformation energy, ΔE_{def}) is marked in the figure.

S8. Protonation of [3]Rotaxanes Monitored by ^{1}H and 2D NMR

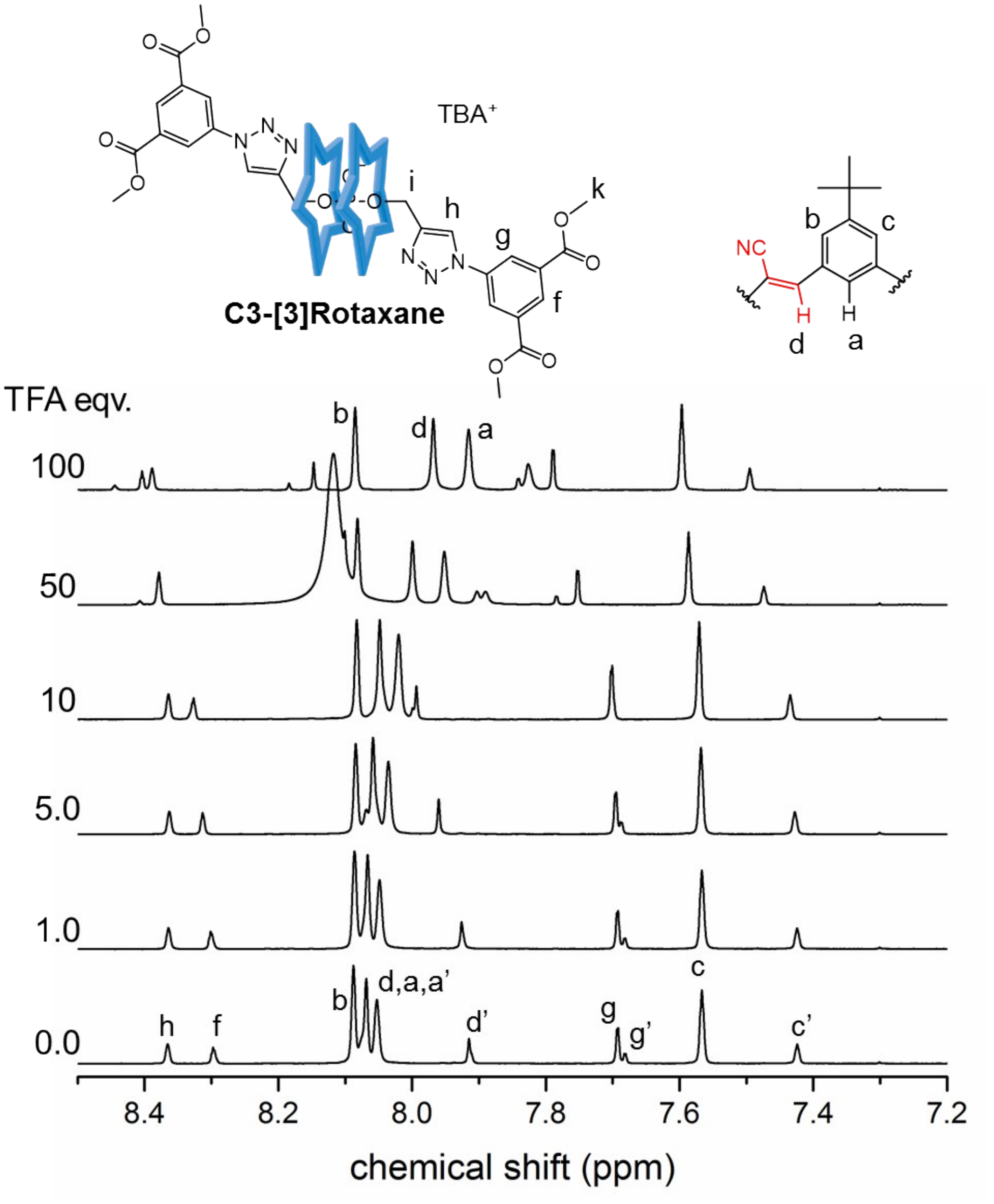

Figure S15. Stacked ^{1}H NMR spectra of TBA•**C3-[3]rotaxane** with increasing amount of TFA (2 mM, CD_2Cl_2, 298 K, 600 MHz).

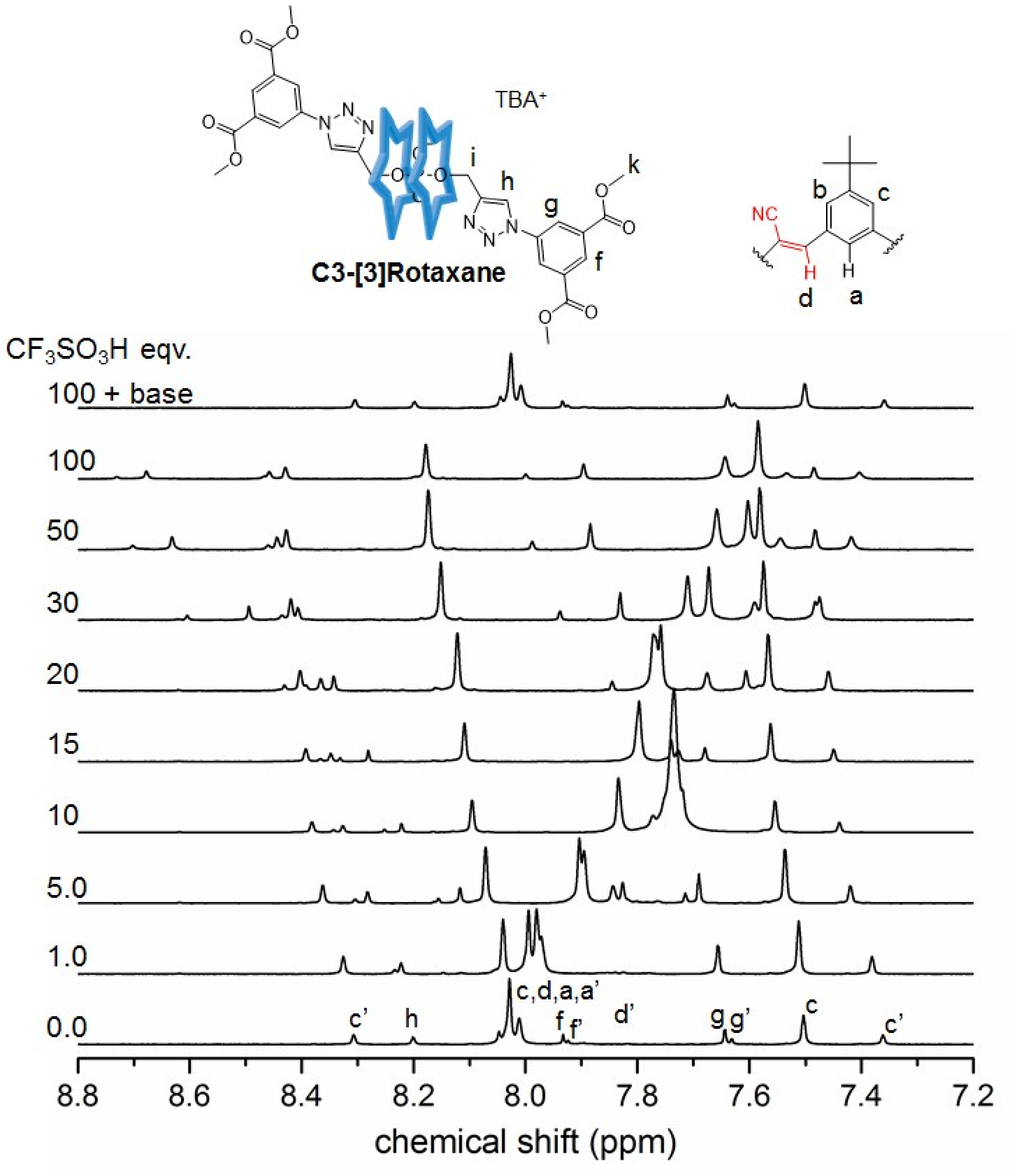

Figure S16. Stacked ^{1}H NMR spectra of TBA•**C3-[3]rotaxane** with increasing amount of triflic acid until 100 equivalents and neutralized by access amount of Et_3N (2 mM, 2:1 CD_2Cl_2:CD_3CN, 298 K, 600 MHz).

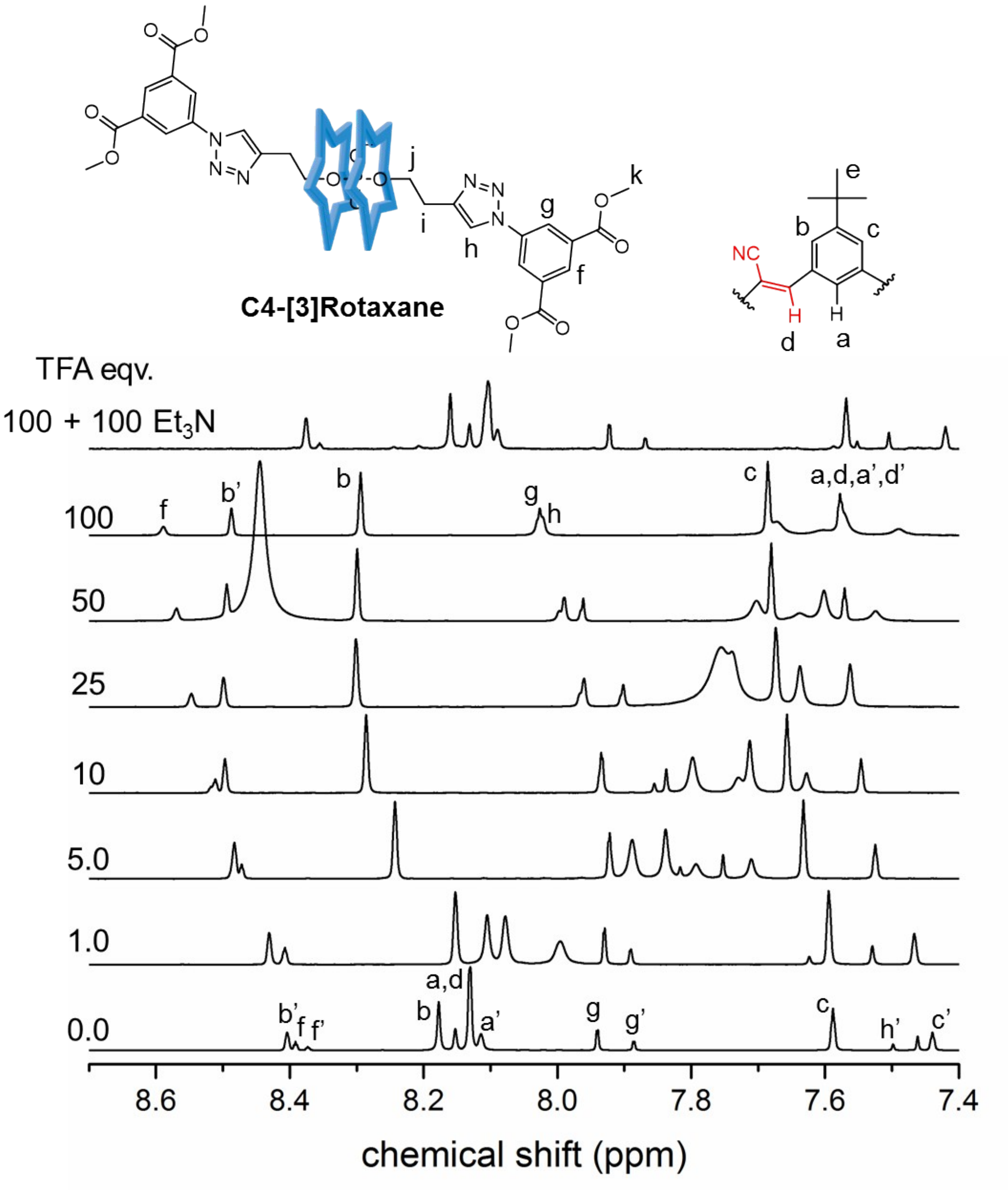

Figure S17. Stacked ^{1}H NMR spectra of TBA•**C4-[3]rotaxane** with increasing amount of TFA until 100 equivalents and neutralized by 100 equivalents of Et_3N (2 mM, CD_2Cl_2, 298 K, 600 MHz).

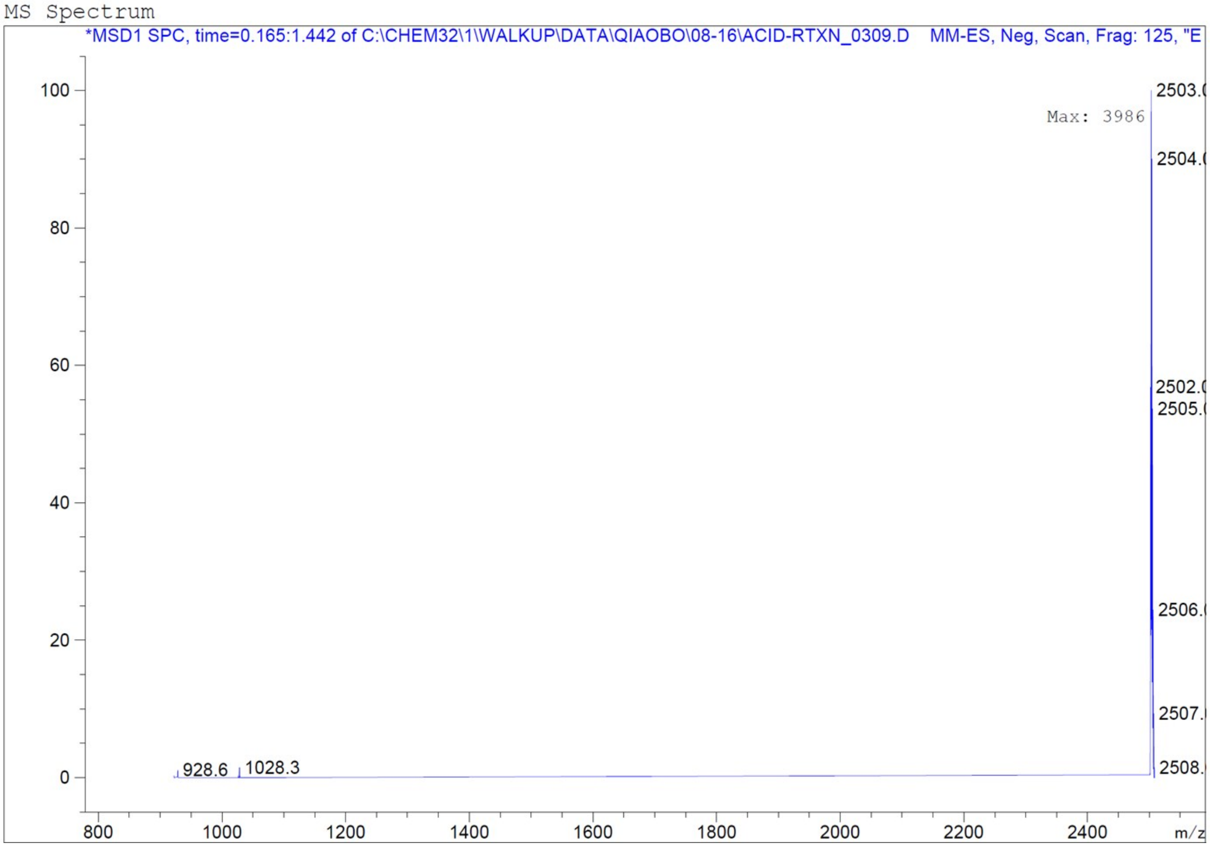

Figure S18. Mass spectroscopy of protonated TBA•**C4-[3]rotaxane** (CH_2Cl_2, 100 equivalents of TFA, ESI).

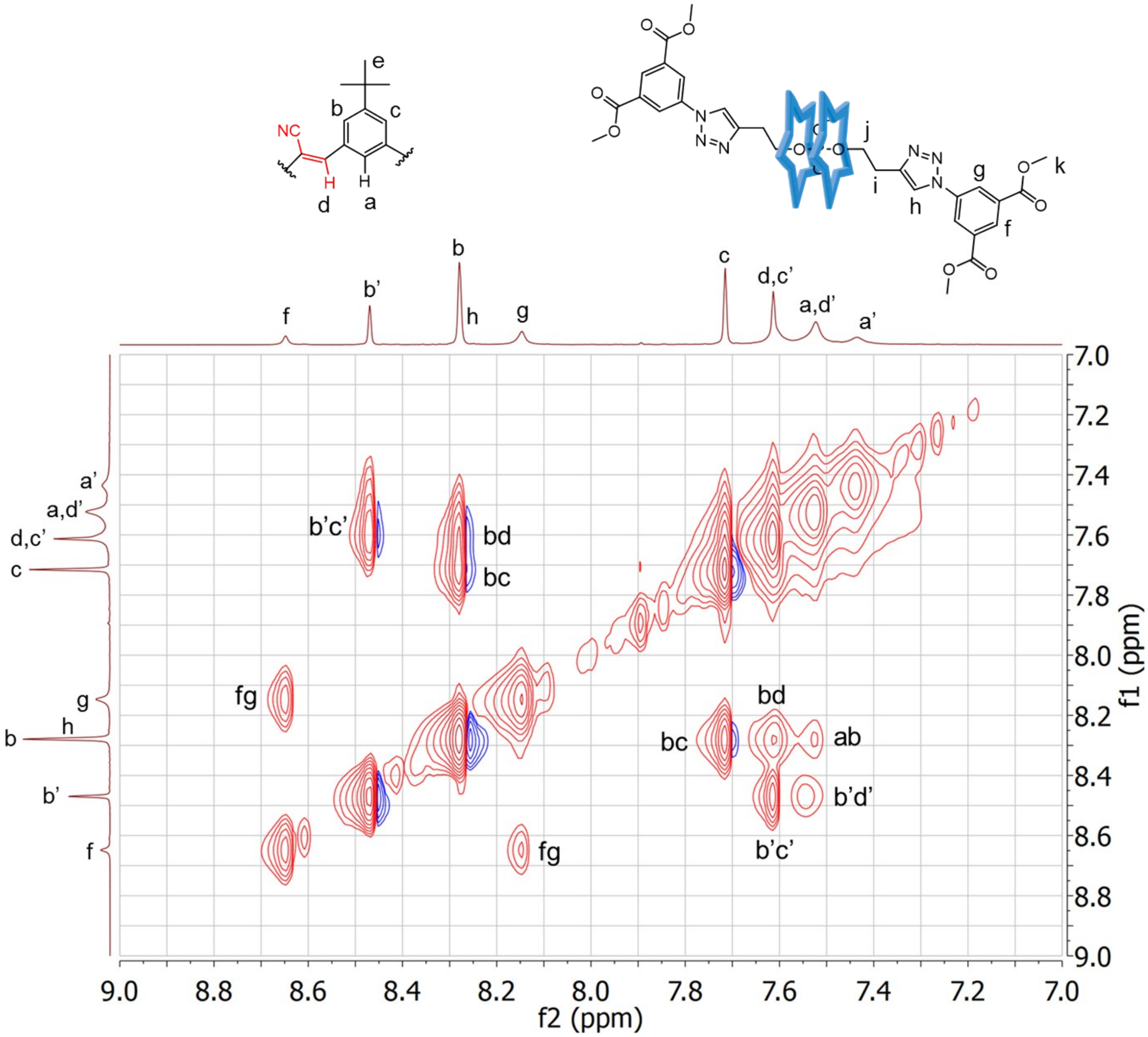

Figure S19. ^{1}H-^{1}H Through-bond coupling TOCSY NMR spectrum of protonated TBA•**C4-[3]rotaxane** (5 mM, 100 equivalents of TFA, CD_2Cl_2, 600 MHz) shows cross peaks for separate spin systems of the major and minor (') diastereomers.

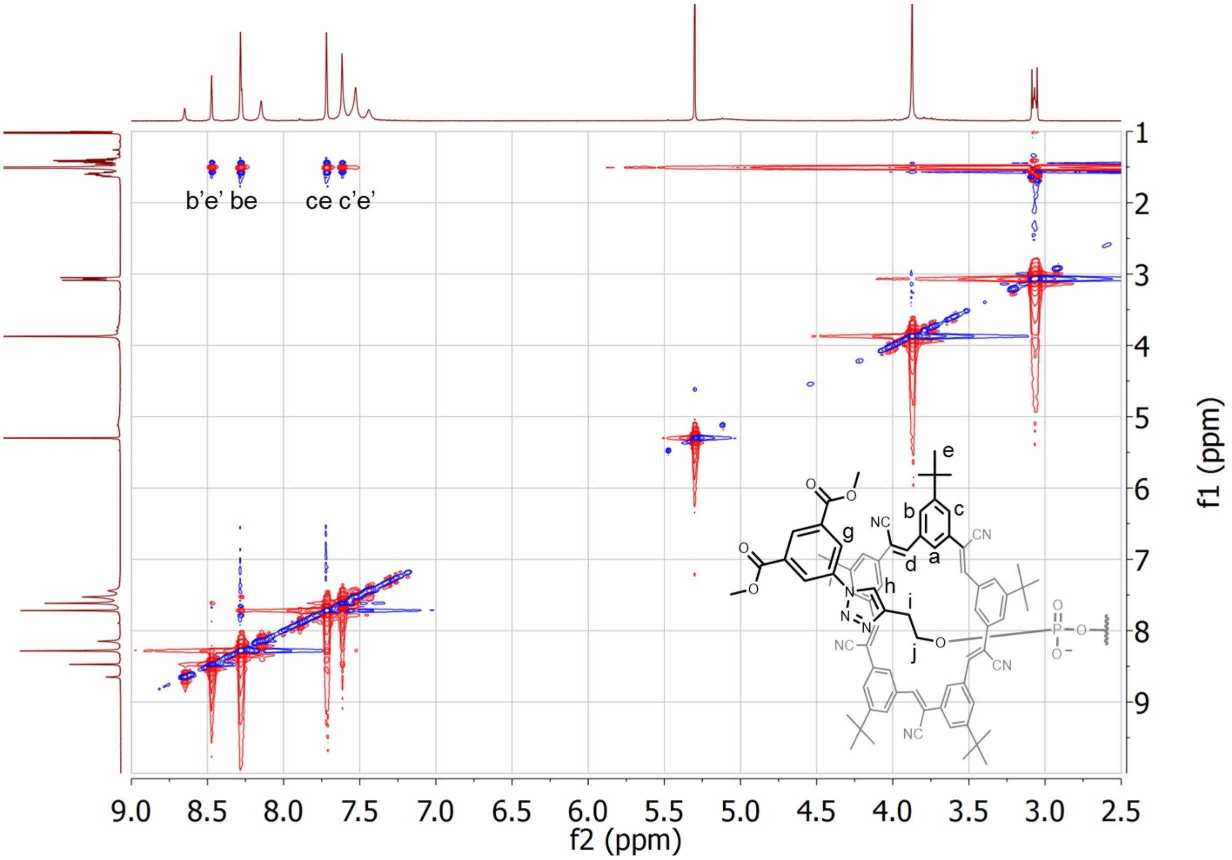

Figure S20. ^{1}H-^{1}H Through-space ROESY NMR spectrum of protonated TBA•**C4-[3]rotaxane** (5 mM, 100 equivalents TFA, CD_2Cl_2, 500 MHz, mixing time: 0.2 s).

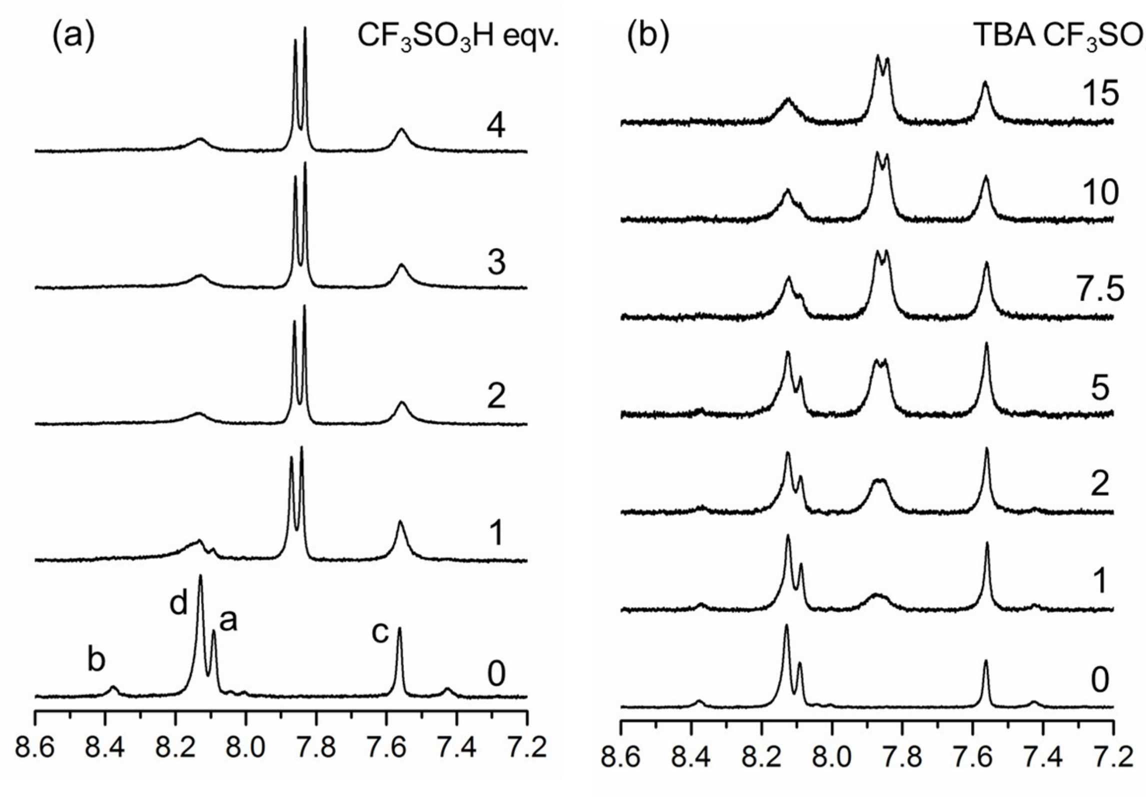

Figure S21. Stacked ^{1}H NMR spectra of a 3:1 mixture of TBA•**P-C3** (3 mM) and cyanostar (1 mM) with increasing amount of (a) triflic acid and (b) TBA triflate (2:1 CD_2Cl_2:CD_3CN, 600 MHz, 298 K).

The binding of **P-C3**$^{-}$ is switched off with the addition of triflic acid and results in cyanostar-triflate complex. However, the addition of TBA triflate as a competitive anion into the same 3:1 mixture does not switch off the binding of **P-C3**$^{-}$.

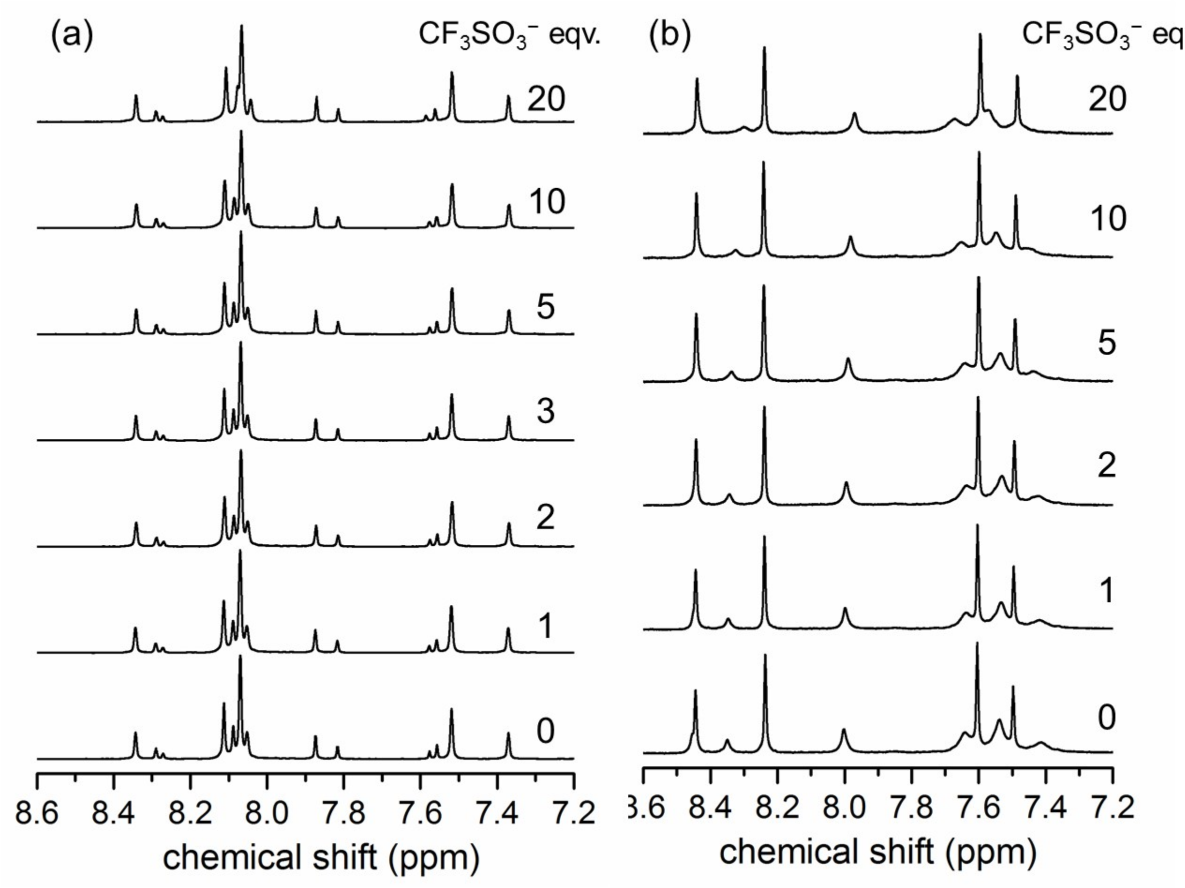

Figure S22. Stacked ^{1}H NMR spectra of (a) neutral **C4-[3]rotaxane** and (b) **C4-[3]rotaxane** and 2 equivalents of triflic acid with increasing amount of TBA triflate (2 mM, 2:1 CD_2Cl_2:CD_3CN, 600 MHz, 298 K).

References

---

1. Lee, S.; Chen, C.-H.; Flood, A. H. *Nat. Chem.* **2013**, *5*, 704-710.
2. Fiala, T.; Sindelar, V. *Supramol. Chem.* **2016**, *1*. 1-7.
3. von Delius, M.; Geertsema, E. M.; Leigh, D. A. *Nat. Chem.* **2010**, *2*, 96–101.
4. SAINT, Bruker Analytical X-Ray Systems, Madison, WI, current version.
5. SADABS, Bruker Analytical X-Ray Systems, Madison, WI, current version.
6. Sheldrick, G. M. *Acta Cryst*. **2008**, *A64*, 112-122.
7. Hirsch, B. E.; Lee, S.; Qiao, B.; Chen, C.-H.; McDonald, K. P.; Tait, S. L.; Flood, A. H. *Chem. Commun.* **2014**, *50*, 9827-9830.
8. Spek, A. L. *Acta Cryst*. **2015**, *C71*, 9-18.
9. Bondi, A. *J. Phys. Chem*. **1964**, *68*, 441-451.

---

10. Zhao, Y.; Truhlar, D. G. *Theor. Chem. Acc.* **2008**, *120*, 215.

11. Spartan ’14 Wavefunction, Inc. Irvine, CA.

12. Halgren, T. A. *J. Comp. Chem.* **1996**, *17*, 490.